AD NUMBER

AD451430

NEW LIMITATION CHANGE

TO

Approved for public release, distribution unlimited

FROM

Distribution authorized to U.S. Gov't. agencies and their contractors; Administrative/Operational Use; OCT 1964. Other requests shall be referred to Navy Underwater Sound Laboratory, New London, CT.

AUTHORITY

CESTI per USNUSL ctr, 17 Dec 1965

AD 451430

51

USL Report No. 622
USL Project No. 1-450-00-00

DYNAMIC COUPLING COEFFICIENTS FOR DISTRIBUTED PARAMETER PIEZOELECTRIC TRANSDUCERS

S-F001 03 18-8044

16 October 1964

by
William J. Marshall

U. S. NAVY UNDERWATER SOUND LABORATORY
FORT TRUMBULL, NEW LONDON, CONNECTICUT

ABSTRACT

This report discusses a definition of the effective coupling coefficient for the body-force class of electromechanical transducers. This definition is based on the distribution of energy in the transducer and is therefore particularly applicable to the "distributed parameter" type of transducer. Furthermore, the definition results in a frequency dependent coupling coefficient which is valid for all modes of vibration.

The definition is applied to some common types of longitudinal vibrator and the results are compared with experiments for one particular device (a partially excited stack of ceramic discs). The influence of parasitic elements on the system coupling is also examined.

ADMINISTRATIVE INFORMATION

The work covered by this report was accomplished under USL Project No. 1-450-00-00 and Navy Subproject and Task No. S-F001 03 18-8044.

REVIEWED AND APPROVED: 16 October 1964

H. E. Nash
Technical Director

R. L. Corkran, Jr., Captain, USN
Commanding Officer and Director

TABLE OF CONTENTS

LIST OF ILLUSTRATIONS

TABLE

DYNAMIC COUPLING COEFFICIENTS FOR DISTRIBUTED PARAMETER PIEZOELECTRIC TRANSDUCERS

INTRODUCTION

Distributed parameter transducers may be described with some success by analogous circuits containing frequency-dependent circuit elements, but the extraction of an effective coupling coefficient from such a circuit is usually done with approximation techniques which have doubtful validity for devices with high material coupling.

This report exploits a definition of the effective coupling based on the distribution of energy in the vibrating system and applies it to various specific transducers. This definition not only produces exact values of the coupling factor for all frequencies and modes; it also sheds light on the somewhat enigmatic "meaning" of the coupling coefficient concept for composite transducers.

In this report, the development begins with a derivation of the equations of motion, followed by a complete electromechanical description of three types of distributed parameter transducers (all of the "longitudinal vibrator" class). This work, of course, is available in many places in the literature; it is reproduced here to establish nomenclature for the main body of the report.

The third section introduces the definition of coupling to be used and applies it to the three transducers described in the preceding section. A general discussion of coupling coefficients for composite transducers follows. A theoretical description of a partially excited longitudinal vibrator is compared with experimental data in the final section.

The transducers considered in the report are all piezoelectrically excited, but the concept applies equally well to the magnetostrictive devices.

DERIVATION OF THE LONGITUDINAL VIBRATOR EQUATIONS

THE CONSTANT FIELD LONGITUDINAL VIBRATOR

Consider a segmented longitudinal vibrator of length 2ℓ which vibrates in the x-direction symmetrically about its center. The lateral dimensions of the bar are small compared to ℓ so that lateral vibrations are ignored and the shape of the cross-sectional area, A, is arbitrary (rectangular, circular, and annular shapes are common). The deflection $\xi(x)$ of the plane at position x, and the stress at this point, $T(x)$, obey the differential equation

$$\rho\omega^2\xi(x) + \frac{\partial T(x)}{\partial x} = 0 \tag{1}$$

for harmonic excitation at angular frequency ω. The density of the material is ρ.

Numerous electrodes placed in the y-z plane and evenly spaced with separation t along the x-axis produce an electric field whose x component is $\mathcal{E}(x)$ and an electric displacement with x component $D(x)$. The electrodes are connected in parallel in the usual fashion. These electric variables are connected with the stress and the strain, $S(x)$, by the following piezoelectric equations of state:

$$\begin{cases} S(x) = s_{33}^{E} T(x) + d_{33}\,\mathcal{E}(x) \\ D(x) = d_{33} T(x) + \epsilon_{33}^{T}\,\mathcal{E}(x). \end{cases} \tag{2}$$

The strain is the gradient of the deflection, $S = \partial\xi/\partial x$. Assuming that the electrodes are spaced so closely that the electric field strength does not vary along the length of the material ($\partial\mathcal{E}/\partial x = 0$), Eq. (1) becomes the familiar Helmholtz Equation:

$$\frac{\partial^2\xi(x)}{\partial x^2} + \omega^2\rho s_{33}^{E}\xi(x) = 0. \tag{3}$$

The general solution of Eq. (3) is

$$\xi(x) = B_1 \sin kx + B_2 \cos kx , \tag{4}$$

where the wave number $k = \omega/c_3^E$, and the speed of sound in the material at constant field is $c_3^E = (\rho s_{33}^E)^{-1/2}$. Applying the boundary conditions on ξ:

$$\left.\begin{aligned} \xi(0) &= 0 \\ \xi(\ell) &= \xi_0 \end{aligned}\right\} \tag{5}$$

results in the exact solution of the differential equation,

$$\xi(x) = \xi_0 \frac{\sin kx}{\sin k\ell} , \tag{6}$$

and, immediately, the distribution of strain:

$$S(x) = \frac{\partial \xi}{\partial x} = \xi_0 k \frac{\cos kx}{\sin k\ell} . \tag{7}$$

Use of the first equation of state now gives the stress distribution in the vibrator:

$$T(x) = \frac{1}{s_{33}^E} \left(\xi_0 k \frac{\cos kx}{\sin k\ell} - d_{33} \mathcal{E}_0 \right) \tag{8}$$

(The subscript on $\mathcal{E}$ is a reminder that the field is now regarded as a spatial constant.)

If the ends of the sample are free [$T(\ell) = 0$], Eq. (8) establishes the relation between the two amplitude parameters, ξ_0 and $\mathcal{E}_0$:

$$\xi_0 k \cot k\ell = d_{33} \mathcal{E}_0 . \tag{9}$$

The resonant frequencies of the longitudinal vibrator depend on the electrical terminations. If the terminals of the transducer are short-circuited, the natural frequencies are found from Eq. (9) with $\mathcal{E}_0 = 0$:

$$\left.\begin{aligned} &\cot k^E \ell = 0 \\ &k^E \ell = m\frac{\pi}{2}; \quad m = 1, 3, 5, \ldots \end{aligned}\right\} \tag{10}$$

(The superscript E indicates constant voltage conditions.) The current flow between two electrodes is

$$i_n = j\omega A D_n \tag{11}$$

where D_n is the value of the displacement current in the region between x_n and x_{n-1}. The total current flow is the sum of the i_n's:

$$i = j\omega A \Sigma D_n = j\omega A \left(\frac{\ell}{t}\right) D_{av} \tag{12}$$

$$= j\omega A \left(\frac{\ell}{t}\right) \frac{1}{\ell} \int_0^\ell D(x)\,dx . \tag{13}$$

Under the many-electrode assumption ($\ell/t \gg 1$), $D(x)$ may be regarded as a continuous function of x. It is obtained by inserting Eq. (8) in the second equation of state:

$$D(x) = \frac{d_{33}}{s^E_{33}} \xi_o k \frac{\cos kx}{\sin k\ell} + \epsilon^T_{33} \left(1 - \frac{d^2_{33}}{s^E_{33}\epsilon^T_{33}}\right) \mathcal{E}_o . \tag{14}$$

Recognizing the material coupling coefficient

$$k^2_{33} = \frac{d^2_{33}}{s^E_{33}\epsilon^T_{33}} \tag{15}$$

and performing the integration of Eq. (13) results in the total current

$$i = j\omega \frac{A}{t} \left[\frac{d_{33}}{s^E_{33}} \xi_o + \epsilon^T_{33} (1 - k^2_{33}) \mathcal{E}_o \ell\right] . \tag{16}$$

Under open-circuit conditions, there is no current flow. Putting Eq. (16) equal to zero yields the open-circuit deflection/field relationship which must coexist with Eq. (9). Combining these two produces the equation for the allowed frequencies at constant current:

$$k^I \ell \cot k^I \ell = -\frac{k^2_{33}}{1 - k^2_{33}} . \tag{17}$$

The open-circuit voltage is simply

$$V_{o.c.} = \mathcal{E}_o t = -\frac{k_{33}^2}{1-k_{33}^2}\ \frac{\xi_o}{d_{33}}\left(\frac{t}{\ell}\right). \tag{18}$$

Examination of Eqs. (10) and (17) shows that the short-circuited frequencies (constant voltage resonances) depend only on elastic constants and dimensions, while the open-circuited frequencies (constant voltage anti-resonances) depend also on the piezoelectric properties of the material as indicated by the presence of k_{33} in Eq. (17). Furthermore, if one measures the fundamental (m = 1) resonance and anti-resonance of an unloaded stack, the material coupling may be found by forming the ratio $r = \omega^1/\omega^2$ and noting that

$$k^1\ell - rk^2\ell = r\frac{\pi}{2}. \tag{19}$$

Now Eq. (17) becomes[1]

$$-\frac{k_{33}^2}{1-k_{33}^2} = r\frac{\pi}{2}\cot r\frac{\pi}{2}. \tag{20}$$

The electrical admittance of the device is found by dividing the current in Eq. (16) by the voltage, $\mathcal{E}_o t$:

$$Y_o = \frac{i}{\mathcal{E}_o t} = j\omega A\,\frac{\epsilon_{33}^T \ell}{t^2}\left[k_{33}^2\,\frac{\tan k\ell}{k\ell} + 1 - k_{33}^2\right]. \tag{21}$$

Because this analysis considers a lossless system, the electrical admittance is entirely imaginary. Rewriting Y_o in the form

$$Y_o = j\left\{\omega A\,\frac{\epsilon_{33}^T \ell}{t^2}\ k_{33}^2\,\frac{\tan k\ell}{k\ell} + \omega\,\frac{\epsilon_{33}^T \ell}{t^2}\ A(1-k_{33}^2)\right\} \tag{22}$$

shows that the admittance has the form of two susceptances in parallel. The second term represents the susceptance of a capacitor of value

$$C_o = \frac{A\ell\,\epsilon_{33}^T}{t^2}(1-k_{33}^2), \tag{23}$$

---

[1] This equation is a well-known relation between material coupling and the resonant-to-anti-resonant frequency spread. See: Berlincourt et al., Proc. Institute of Radio Engineers, vol. 48, p. 220.

while the first term is called the motional susceptance. By introducing the characteristic mechanical impedance of the material, $Z_c = \rho cA$, this motional susceptance takes the form

$$B_{mot} = \frac{(Ad_{33}/s^E_{33}t)^2}{-jZ_o \cot kl} = \frac{N^2}{-jZ_o \cot kl} , \qquad (24)$$

where $N = Ad_{33}/s^E_{33}t$ is called electromechanical transformation ratio. An equivalent circuit which has the admittance Y_o at its terminals is shown in Fig. 1.

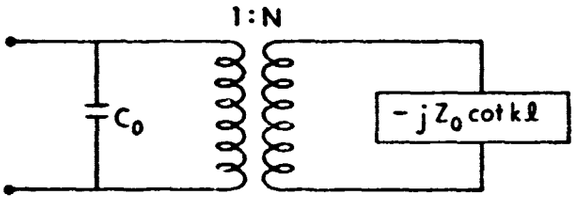

Fig. 1 - Equivalent Circuit of the Constant Field Longitudinal Vibrator

Examination of Eq. (21) shows that the resonant frequencies defined by Eq. (10) — the constant voltage resonances — cause $Y_o = \infty$, while those frequencies defined by Eq. (17) — the constant current resonances — produce $Y_o = 0$.

The capacitance C_o is called the blocked capacitance. It may be interpreted as the capacity of the segmented bar when it is clamped to prevent motion; the dielectric constant applicable for this calculation is designated "longitudinally clamped": $\epsilon^{LC} = \epsilon^T_{33}(1 - k^2_{33})$.

The analysis of a thin bar in longitudinal vibration due to transverse electric fields ("31" mode of operation) follows the form of the preceding theory closely; the "31" subscript replaces the "33" on all material constants. The reason for the similarity is that both methods of excitation share the common characteristic that the electrically produced strain is uniform in the direction of motion. This is achieved in the "33" case by using closely spaced electrodes placed normal to the $\hat{\mathcal{E}}$ vector and in the "31" case by using continuous electrodes along the sides of the bar.

If, however, a bar vibrates so that an appreciable portion of the acoustic wavelength fits between the electrodes, there will be a variation

of field in this interval. This may occur for higher modes of the "33" vibrator just discussed (large m), or for the fundamental mode of a column of ceramic with electrodes only on the ends ($x = \pm \ell$) and none within the material (i.e., a solid, rather than segmented, stack). Such electromechanical behavior is characterized by $\partial \mathcal{E}/\partial x \neq 0$ (spatially variable field) and is described in the next part of the report.

THE VARIABLE FIELD
LONGITUDINAL VIBRATOR

The analysis of this type of vibration parallels that just discussed. The same geometry and coordinate system are used, but it is appropriate to employ a different set of Equations of State:

$$\begin{cases} S(x) = s_{33}^{D} T(x) + g_{33} D(x) \\ \mathcal{E}(x) = -g_{33} T(x) + \beta_{33}^{T} D(x) . \end{cases} \tag{25}$$

It is interesting to see how the material constants with superscript D are related to those with superscript E. For constant D (or D = 0), Eq. (2) becomes

$$\begin{cases} S = s_{33}^{E} T + d_{33} \mathcal{E} \\ 0 = d_{33} T + \epsilon_{33}^{T} \mathcal{E} . \end{cases} \tag{26}$$

Eliminating $\mathcal{E}$ from this pair yields

$$S = s_{33}^{E} \left(1 - \frac{d_{33}^{2}}{s_{33}^{E} \epsilon_{33}^{T}} \right) T . \tag{27}$$

This is Hooke's Law for the constant D case; the elastic constant is smaller than s_{33}^{E} and is

$$s_{33}^{D} = s_{33}^{E} (1 - k_{33}^{2}) . \tag{28}$$

The electric constant β^{T} appearing in Eq. (25) is the reciprocal of the permittivity of the material, ϵ^{T}. The piezoelectric constant g is related to d by

$$g_{33} = d_{33}/\epsilon_{33}^{T} . \tag{29}$$

The first of Eq. (25) is inserted in the general differential equation, Eq. (1). The resulting equation is simplified by recognizing that, although $\mathcal{E}$ may have spatial variations along the x axis of the bar, the electric displacement must be constant and thus $\partial D/\partial x = 0$.

The two electrical conditions are, as before, constant voltage and constant current. The first relation is obtained by making the total voltage developed across the two electrodes vanish:

$$E = \int_0^{\ell} \mathcal{E}(x)\, dx = 0. \tag{30}$$

The open-circuit conditions are established by making D = 0. The two sets of natural frequencies that result are found from:

$$\begin{cases} \text{short circuited:} & \kappa^E \ell \cot(\kappa^E \ell) = k_{33}^2 & (31) \\ \text{open circuited:} & \cot(\kappa^I \ell) = 0 & (32) \end{cases}$$

The wave numbers κ^E and κ^I are different from those in the preceding section since different elastic constants are used for this type of vibration:

$$(\kappa^E = \omega^E / c_3^D \ , \ \kappa^I = \omega^I / c_3^D).$$

Note that the constant voltage resonances depend on coupling and the constant current frequencies do not. This is the reverse of the behavior of the segmented bar described in the preceding section.

A circuit which has the same electrical impedance as the vibrator is shown in Fig. 2.

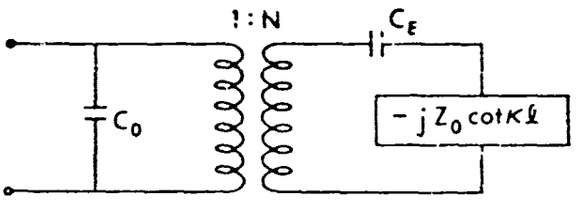

Fig. 2 - Equivalent Circuit of the Variable Field Longitudinal Vibrator

The values of the circuit elements are

$$C_o = \frac{A\epsilon_{33}^T}{2\ell}(1-k_{33}^2), \qquad N = \frac{Ad_{33}}{2s_{33}^D\ell}, \qquad C_2 = -\frac{C_o}{N^2}.$$

The frequencies which satisfy Eqs. (31) and (32) make the admittance of this circuit infinite and zero, respectively. Equation (31) shows that the constant voltage resonances are displaced below their values in the $\partial\mathcal{E}/\partial x = 0$ case; the overtones are not integral multiples of the fundamental.

This is represented graphically in Fig. 3 where $(\tan\kappa\ell)$ and $(\kappa\ell/k_{33}^2)$ are plotted against $\kappa\ell$; the intersections of the two curves represent the natural frequencies.

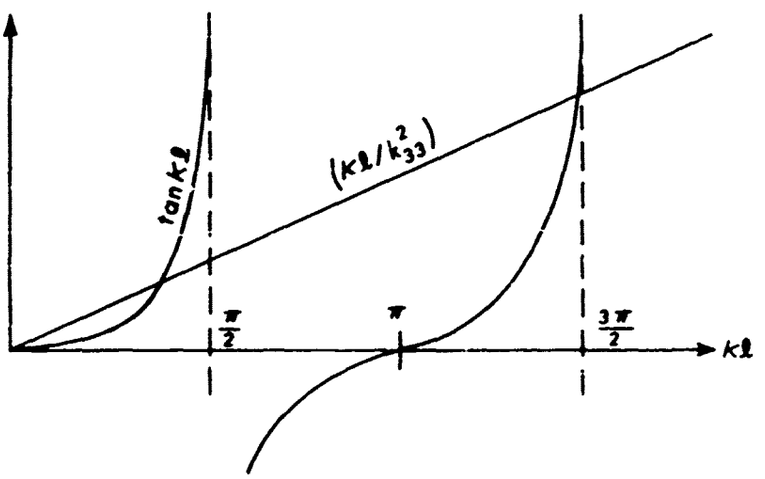

Fig. 3 - Graphical Representation of Eq. (31) (see text)

Note that the roots are displaced from the lower modes,[2] but approach even overtones for large $(\kappa\ell)$.

Furthermore, for low values of the material coupling coefficient k_{33}, the slope of the straight line increases rapidly, and the frequency displacements become small even for the lower modes.

[2] This behavior occurs also for shear modes. See: H. F. Tiersten, Journal of the Acoustical Society of America, vol. 35, p. 53, January 1963.

By measuring the ω^E and ω^I for the fundamental mode and forming the ratio $r = \omega^I/\omega^E$, one can determine the material coupling from

$$k_{33}^2 = \frac{\pi/2}{r} \cot\left(\frac{\pi/2}{r}\right) . \tag{33}$$

This equation, and its companion for the segmented bar Eq. (20), assume a more familiar form by using the notation $f^I = f^E + \Delta f$. Then[3]

$$\left\{ \begin{array}{l} \text{Segmented Bar:} \\ (\partial \mathcal{E}/\partial x = 0) \end{array} \right. \qquad \frac{k_{33}^2}{1 - k_{33}^2} = \frac{\pi}{2}\left(1 + \frac{\Delta f}{f^E}\right) \tan\left(\frac{\pi}{2}\,\frac{\Delta f}{f^E}\right) \tag{34}$$

$$\left\{ \begin{array}{l} \text{End-electroded Bar.} \\ (\partial D/\partial x = 0) \end{array} \right. \qquad k_{33}^2 = \frac{\pi}{2}\left(1 - \frac{\Delta f}{f^I}\right) \tan\left(\frac{\pi}{2}\,\frac{\Delta f}{f^I}\right) \tag{35}$$

These relations are illustrated in Fig. 4.

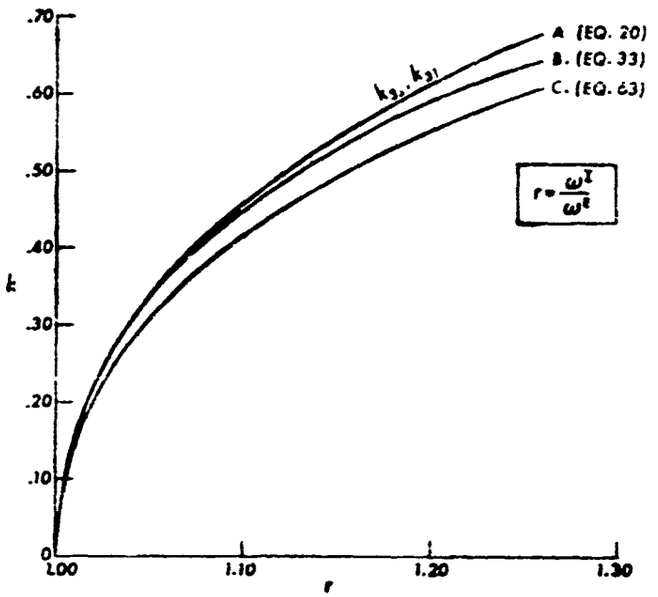

Fig. 4 - Ceramic Material Coupling Coefficients as Determined from the Ratio of Anti-Resonant to Resonant Frequencies for. A. Segmented Bar and Side-Electroded Bar ($\partial \mathcal{E}/\partial x = 0$), B. End-Electroded Bar ($\partial D/\partial x = 0$); and C. Effective Coupling for Lumped Constant Transducer

---

[3] Berlincourt, op.cit.(footnote 1).

Equation (34) may also be used to find k_{31} for samples with their electrodes parallel to the displacement. This is because $\partial \mathcal{E}/\partial x = 0$ is satisfied for side-electroded bars also.

THE PARTIALLY EXCITED LONGITUDINAL VIBRATOR

The type of vibration discussed in this section results if the segmented bar is driven with a given number of the electrodes on either end disconnected so that only the central portion of the bar (symmetrically located about the origin) is electrically excited.

Clearly the ceramic's elastic properties are different in the two regions; therefore, the wave equation must be solved separately in each portion of the bar and the additional constants eliminated by joining the two solutions at the point of discontinuity.

Let the parameter γ designate the fraction of the bar that is excited electrically $(0 \leq \gamma \leq 1)$, and let the subscripts "d" and "f" designate the driven portion $(|x| < \gamma \ell)$ and the free portion $(\gamma \ell < |x| < \ell)$, respectively. The equations of state, Eq. (2), apply to the d-section and those of Eq. (25) to the f-section. In using Eq. (25) it should be recalled that

$$D(x) = 0 \quad \text{for} \quad \ell > x > \gamma \ell ,$$

since those electrodes are disconnected from each other. If the electrodes in the f-region were tied together but not connected to the electrical generator, a different sort of motion would result, but that case is not considered here.

The analysis in the d-section follows the derivation of the constant field longitudinal vibrator up to the equation for the displacement function, Eq. (4). Making the vibration symmetrical about the origin with $\xi_d(0) = 0$ and specifying the displacement at the plane of discontinuity, $\xi_d(\gamma \ell) = \xi_\gamma$, yields the particular solution

$$\xi_d(x) = \xi_\gamma \frac{\sin K_d x}{\sin \gamma \Lambda_d} , \tag{36}$$

where the wave number K_d applies only to the d-region,

$$K_d = \frac{\omega}{c_3^E} , \tag{37}$$

and

$$\Lambda_d = K_d \ell . \tag{38}$$

Differentiating Eq. (36) produces the strain function; this is then combined with the first equation of state to get the stress distribution in the d-section of the bar:

$$T_d(x) = \frac{1}{s_{33}^E} \left(\xi_\gamma K_d \frac{\cos K_d x}{\sin \gamma \Lambda_d} - d_{33} \mathcal{E}_0 \right) . \tag{39}$$

A procedure similar to the above is used to find $\xi_f(x)$ and $T_f(x)$. The boundary conditions used are:

a. Matching displacements at the γ interface: $\xi_f(\gamma\ell) = \xi_\gamma$.

b. Unloading the free end: $T_f(\ell) = 0$.

The results are

$$\xi_f(x) = \xi_\gamma \frac{\cot \Lambda_f \cos K_f x + \sin K_f x}{\cot \Lambda_f \cos \gamma \Lambda_f + \sin \gamma \Lambda_f} \tag{40}$$

and

$$T_f(x) = \frac{K_f \xi_\gamma}{s_{33}^D} \frac{\cos K_f x - \cot \Lambda_f \sin K_f x}{\cos \gamma \Lambda_f (\cot \Lambda_f + \tan \gamma \Lambda_f)} , \tag{41}$$

where the wave number K_f is ω / c_3^D and $\Lambda_f = K_f \ell$. The remaining condition on the two solutions is that of matching the stresses at $x = \gamma\ell$. Since there are no more undetermined constants in the problem, this operation will produce a fixed relation between the two amplitude-determining parameters, ξ_γ and $\mathcal{E}_0$. The resulting equation is the analog of Eq. (9) for the partially excited bar:

$$\xi_\gamma \left(\frac{K_f}{s_{33}^D} \frac{1 - \cot \Lambda_f \tan \gamma \Lambda_f}{\cot \Lambda_f + \tan \gamma \Lambda_f} - \frac{K_d}{s_{33}^E} \cot \gamma \Lambda_d \right) = - \frac{d_{33}}{s_{33}^E} \mathcal{E}_o . \tag{42}$$

The natural frequencies of vibration when the electric terminals are short-circuited are those which satisfy Eq. (42) when $\mathcal{E}_o = 0$. Designating the allowed values of Λ_d for this condition by the superscript E (constant voltage), and using the relation $\Lambda_f = \Lambda_d \sqrt{1 - k_{33}^2}$ and the trigonometric identity

$$\frac{\cot \gamma \Lambda - \cot \Lambda}{\cot \gamma \Lambda \cot \Lambda + 1} = \tan (1 - \gamma) \Lambda ,$$

one obtains the following implicit relation for Λ_d^E as a function of γ :

$$\left[\tan (1 - \gamma) \sqrt{1 - k_{33}^2} \; \Lambda_d^E \right] \tan \gamma \Lambda_d^E = \sqrt{1 - k_{33}^2} . \tag{43}$$

The constant current resonances are found by making $\int_o^{\gamma \ell} D \, dx = 0$. The distribution of electric displacement along the bar is found from the second equation of state:

$$\begin{aligned} D_d(x) &= \epsilon_{33}^T \mathcal{E}_o + d_{33} T_d(x) \\ &= \epsilon_{33}^T \mathcal{E}_o (1 - k_{33}^2) + \frac{d_{33} \xi_\gamma K_d}{s_{33}^E} \frac{\cos K_d x}{\sin \gamma \Lambda_d} \end{aligned} \Bigg\} . \tag{44}$$

Performing the integration and equating the result to zero yields the open-circuit voltage/deflection relation:

$$s_{33}^E \epsilon_{33}^T \mathcal{E}_o (1 - k_{33}^2) + d_{33} \xi_\gamma = 0 . \tag{45}$$

This result is combined with the fixed $\xi_\gamma / \mathcal{E}_o$ relation given in Eq. (42) to obtain the open-circuit resonances.

$$\gamma \Lambda_d^I \left(\cot \gamma \Lambda_d^I - \frac{1}{\sqrt{1-k_{33}^2}} \tan (1-\gamma) \sqrt{1-k_{33}^2}\ \Lambda_d^I \right) = -\frac{k_{33}^2}{1-k_{33}^2} \,. \qquad (46)$$

Equations (43) and (46) reduce to Eqs. (10) and (17), respectively, when $\gamma = 1$. Combining Eqs. (43) and (46) to obtain an expression for k_{33} in terms of the resonant to anti-resonant frequency spread is a more formidable chore than it was for the fully excited cases treated earlier. Furthermore, it is doubtful that the result of such work would be very useful since it is unlikely that knowledge of k_{33} would be sought with experiments on partially excited bars. It is instructive, however, to observe the variations of ω^I and ω^R with γ. The values of these two frequencies for $\gamma = 1$ serve as convenient normalizing values and one may examine the dimensionless ratios

$$\delta^R(\gamma) = \frac{\omega^R(\gamma)}{\omega^R(1)} \qquad (47)$$

and

$$\delta^I(\gamma) = \frac{\omega^I(\gamma)}{\omega^I(1)} \,. \qquad (48)$$

With this notation and Eqs. (10) and (17), the γ-dependent Λ variables become

$$\Lambda_d^R(\gamma) = (\pi/2)\, \delta^R(\gamma) \qquad (49)$$

$$\Lambda_d^I(\gamma) = r\,(\pi/2)\, \delta^I(\gamma) \qquad (50)$$

The solutions of Eqs. (43) and (46) for $\delta^R(\gamma)$ and $\delta^I(\gamma)$ appear in Fig. 5 for the specific case $k_{33} = 0.64$ ($r = 1.22$). The constant current solution is displaced upward by the factor r on the graph so that the curves refer all relative frequencies to $\omega^R(1)$.

Toulis has published data from an experiment involving a partially excited stack[4] with an $r = 1.22$ for $\gamma = 1$. These data are

---

[4] W. J. Toulis, "Redefinition of Effective Electromechanical-Coupling Factor," Journal of the Acoustical Society of America, 35, no. 12, p. 2024, November 1963.

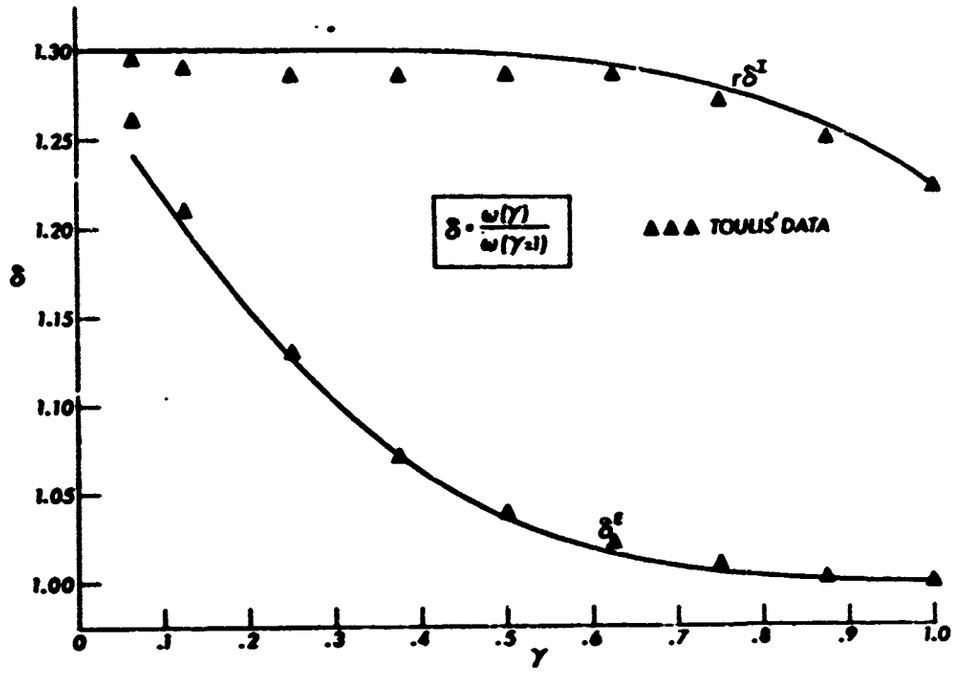

Fig. 5 - δ^E and $r\delta^I$ versus γ for $k_{33} = 0.64$ ($r = 1.22$)

superimposed on the curves of Fig. 5. The failure of the experimental anti-resonant frequencies to coincide with the theoretical curve may be due to the fact that the measurement of anti-resonant frequencies is generally more difficult than resonant frequencies and mechanical losses (which were ignored in the analysis) are more influential at ω^I.

THE ELECTROMECHANICAL COUPLING COEFFICIENT

THE QUASI-STATIC CASE

In the introductory sections of Hersh's excellent report on coupling[5] there are listed for review many familiar definitions of the coupling coefficient. Many of these definitions concentrate on extending the coupling concept from electrical circuit analysis to the realm of electromechanical devices. Such techniques are indeed useful since the description of electromechanical devices through the use of equivalent circuits is a popular method of analysis. In the opinion of this writer, however, these extensions lose much of their usefulness when applied to distributed parameter transducers, since the circuits which describe such devices often contain frequency-dependent elements.

This objection causes one to examine another class of definitions: those which seek to describe coupling in terms of the distribution of electrical and mechanical energies in the transducer. One definition from this group which has particular applicability to the distributed parameter transducers examined in this report is that described by Vigoureux and Booth,[6] Skudrzyk,[7] and Beckmann.[8] This view of coupling is also exploited by Berlincourt et al. in their contribution to the recent book, Physical Acoustics.[9]

The distinguishing feature of this approach is that it considers the total energy of the transducer system to be the sum of three terms: the purely electrical and purely mechanical energies without coupling, and the mutual (or shared) energy resulting from coupling. The square of the coupling coefficient for a particular mode is proportional to the square of the mutual energy divided by the product of the two self energies.

That this definition follows easily from the linear equations of state for piezoelectric transducers is shown by Beckmann in the following manner

---

[5] John F. Hersh, Coupling Coefficients, Acoustics Research Laboratory, Harvard University, Technical Memorandum no. 40, pp. 4-25, 1957.

[6] P. Vigoureux and C. F. Booth, Quartz Vibrators and Their Applications, H. M. Stationery Office, London, p. 58, 1950.

[7] E. Skudrzyk, Die Grundlagen der Akustik, Springer-Verlag, Wien, p. 485, 1954.

[8] R. Beckmann, "Some Applications of the Linear Piezoelectric Equations of State," I.R.E. Transactions on Ultrasonics Engineering, PGUE-3, pp. 55-59, May 1955.

[9] W. P. Mason, Ed., Physical Acoustics, vol. 1, Part A, Academic Press, New York, p. 189 ff., 1964.

Select a pair of equations of state and write them in the form

$$\begin{cases} S_\lambda = \Sigma\, s^E_{\lambda\mu}\, T_\mu + \Sigma\, d_{m\lambda}\, \mathcal{E}_m \\ D_\rho = \Sigma\, d_{\rho\mu}\, T_\mu + \Sigma\, \epsilon^T_{\rho m}\, \mathcal{E}_m \,. \end{cases} \tag{51}$$

The mechanical energy density in the volume where these equations apply is

$$\frac{1}{2}\Sigma\, S_\lambda T^*_\lambda = \frac{1}{2}\Sigma\, s^E_{\lambda\mu}\, T^*_\lambda T_\mu + \frac{1}{2}\Sigma\, d_{m\lambda}\, T^*_\lambda \mathcal{E}_m = W_1 + W_{12}, \tag{52}$$

while the electrical energy density is

$$\frac{1}{2}\Sigma\, D_\rho \mathcal{E}^*_\rho = \frac{1}{2}\Sigma\, d_{\rho\mu}\, \mathcal{E}^*_\rho T_\mu + \frac{1}{2}\Sigma\, \epsilon^T_{\rho m}\, \mathcal{E}^*_\rho \mathcal{E}_m = W_{12} + W_2, \tag{53}$$

where the asterisk indicates a complex conjugate, W_1 represent the purely elastic energy, W_2 the purely electric energy, and W_{12} the mutual piezoelectric energy. The square of the electromechanical coupling coefficient is

$$k^2 = \frac{W^2_{12}}{W_1 W_2} \,. \tag{54}$$

Equations (52) and (53) are quite complicated in the general form; however, if mechanical and electrical boundary conditions for a particular type of excitation leave only a few of the ST and $\mathcal{E}D$ products non-zero, the coupling coefficient may assume a more simple form.

This may be illustrated by considering a sample with the applied field parallel to the axis of polarization ($\mathcal{E}_3 \neq 0$, $\mathcal{E}_1 = \mathcal{E}_2 = 0$) and all stresses normal to this axis zero ($T_1 = T_2 = 0$, $T_3 \neq 0$). Under quasi-static conditions, T_3 and $\mathcal{E}_3$ are uniform throughout the piece and the applicable equations of state Eq. (51) reduce to Eq. (2):

$$\begin{cases} S_3 = s^E_{33}\, T_3 + d_{33}\, \mathcal{E}_3 \\ D_3 = d_{33}\, T_3 + \epsilon^T_{33}\, \mathcal{E}_3 \,. \end{cases} \tag{55}$$

The energy densities of Eqs. (52) and (53) are now quite simple, and one finds the total to be

$$W = \frac{1}{2}\, s^E_{33}\, T_3^2 + 2\left(\frac{1}{2}\, d_{33}\, T_3 \mathcal{E}_3\right) + \frac{1}{2}\, \epsilon^T_{33}\, \mathcal{E}_3^2 \,. \tag{56}$$

Therefore, from Eq. (54),

$$\left.\begin{aligned} k_{33}^2 &= \frac{\left(\frac{1}{2} d_{33} T_3 \mathcal{E}_3\right)^2}{\left(\frac{1}{2} s_{33}^E T_3^2\right)\left(\frac{1}{2} \epsilon_{33}^T \mathcal{E}_3^2\right)} \\ &= \frac{a_{33}^2}{s_{33}^E \epsilon_{33}^T} \end{aligned}\right\} \qquad (57)$$

The above procedure applies to calculations using the so-called homogeneous equations of state in which the dependent and independent state variables are each intensive or extensive, respectively. As Beckmann points out,[10] if one uses the "mixed" equations of state, the ratio of energies Eq. (54) is not k^2 but rather is $(k^2/(1 - k^2))$. This important point is summarized in Table 1.

Table 1
APPROPRIATE RELATIONS BETWEEN COUPLING COEFFICIENT AND ENERGY RATIO FOR VARIOUS EQUATIONS OF STATE
(The subscript t indicates the transpose of a submatrix in the partitioned state matrix.)

Equations of State Used (in Matrix Form)	$\frac{W_{12}^2}{W_1 W_2}$
$\begin{pmatrix} S \\ D \end{pmatrix} = \begin{pmatrix} s^E & d_t \\ d & \epsilon^T \end{pmatrix} \begin{pmatrix} T \\ \mathcal{E} \end{pmatrix}$ $\begin{pmatrix} T \\ \mathcal{E} \end{pmatrix} = \begin{pmatrix} c^D & -h_t \\ -h & \beta^S \end{pmatrix} \begin{pmatrix} S \\ D \end{pmatrix}$	k^2 (Homogeneous)
$\begin{pmatrix} S \\ \mathcal{E} \end{pmatrix} = \begin{pmatrix} s^D & g_t \\ -g & \beta^T \end{pmatrix} \begin{pmatrix} T \\ D \end{pmatrix}$ $\begin{pmatrix} T \\ D \end{pmatrix} = \begin{pmatrix} c^E & -e_t \\ e & \epsilon^S \end{pmatrix} \begin{pmatrix} S \\ \mathcal{E} \end{pmatrix}$	$\frac{k^2}{1 - k^2}$ (Mixed)

[10] Beckmann, op. cit., p. 76.

DYNAMIC COUPLING COEFFICIENTS

For non-static conditions the energy densities W_1, W_2, W_{12} are integrated over the volume of the transducer to account for the distributions of stress and field which occur in the distributed parameter cases. The total energies thus obtained are then used to form the ratio in Eq. (54).

This procedure will be applied to the three examples of such transducers which have been considered in this report.

In the case of the constant field longitudinal vibrator (the segmented bar) one has for the strain energy, with piezoelectric effects ignored,

$$W_1 = \frac{1}{2} s_{33}^E \int_V T^2 \, dV . \tag{58}$$

For T one may use Eq. (8) with $d_{33} = 0$. Calling $T_o = \xi_o / s_{33}^E$ the stress at the center of the bar, Eq. (58) becomes

$$\left.\begin{aligned} W_1 &= \frac{1}{2} s_{33}^E A \frac{T_o^2 k^2}{\sin^2 k\ell} \int_o^\ell \cos^2 kx \, dx \\ &= \frac{1}{4} \frac{s_{33}^E A k T_o^2}{\sin^2 k\ell} \left[k\ell + \sin k\ell \cos k\ell \right] \end{aligned}\right\} \tag{59}$$

Since the field is constant, the electric energy is simply

$$W_2 = \frac{1}{2} \epsilon_{33}^T \int_V \mathcal{E}_o^2 \, dV = \frac{1}{2} \epsilon_{33}^T A \ell \, \mathcal{E}_o^2 . \tag{60}$$

The mutual energy is

$$\left.\begin{aligned} W_{12} &= \frac{1}{2} d_{33} \int_V T \mathcal{E} \, dV \\ &= \frac{1}{2} d_{33} A \mathcal{E}_\circ \frac{T_\circ k}{\sin k\ell} \int_\circ^\ell \cos kx \, dx \\ &= \frac{1}{2} d_{33} A \mathcal{E}_\circ T_\circ . \end{aligned}\right\} \qquad (61)$$

Now Eq. (54) yields the "dynamic" (or "effective") coupling coefficient

$$\begin{aligned} k_\circ^2 &= \frac{W_{12}^2}{W_1 W_2} = \frac{d_{33}^2}{\epsilon_{33}^T s_{33}^E} \frac{2 \sin^2 k\ell}{k\ell \, (k\ell + \sin k\ell \cos k\ell)} \\ &= k_{33}^2 \left\{ \frac{2 \sin^2 k\ell}{k\ell \, (k\ell + \sin k\ell \cos k\ell)} \right\} . \end{aligned} \qquad (62)$$

This effective coupling is plotted against the mode number, $m = k\ell/(\pi/2)$ for $k_{33} = 0.64$ in Fig. 6 (solid curve). Note that the coupling goes

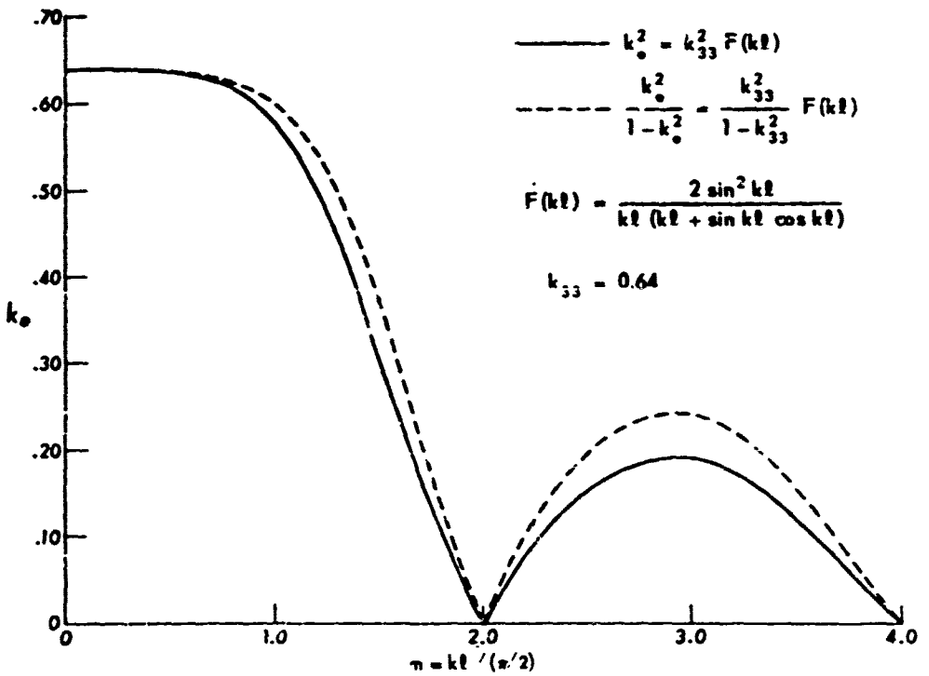

Fig. 6 - Frequency-Dependent Effective Coupling Coefficients for Two Types of Longitudinal Vibrators

to zero for even m since these are prohibited modes of vibration.[11] At zero frequency the effective coupling is equal to the material coupling, k_{33}, since the stress distribution becomes constant.

Of particular interest is k_e at the fundamental resonance:

$$k_e = \sqrt{\frac{8}{\pi^2}}\, k_{33} \quad \text{at} \quad k\ell = \pi/2 .$$

Since there is a constant proportionality between these two factors one could obtain k_e as a function of the frequency spread ratio r by multiplying Curve A in Fig. 4 by $(8/\pi^2)^{1/2} \approx 0.90$. When this is done, however, the resulting curve differs only slightly from the function $k = \sqrt{1 - 1/r^2}$. This latter expression is the effective coupling of a simple lumped constant equivalent circuit for a one-degree-of-freedom transducer; it is usually seen in the form

$$k_e^2 = 1 - (f_r/f_a)^2 . \tag{63}$$

The k_e of Eq. (63) is plotted on Fig. 4 as Curve C.

For the constant D case treated previously (the end-electroded bar), a similar procedure is used to find the dynamic coupling factor. The principal difference is that the mixed equations of state, Eq. (25), are used in the analysis, and therefore Eq. (54) does not apply. The energy densities in an infinitesimal volume element are found by multiplying the equations of state by T and D, respectively.

$$\left.\begin{aligned} \frac{1}{2} TS &= \frac{1}{2} s^D_{33} T^2 + \frac{1}{2} g_{33} DT = W_1 + W_{12} \\ \frac{1}{2} \mathcal{E} D &= -\frac{1}{2} g_{33} TD + \frac{1}{2} \beta^T_{33} D^2 = -W_{12} + W_2 \end{aligned}\right\} \tag{64}$$

Following the rules in Table 1

$$\frac{k_{33}^2}{1 - k_{33}^2} = \frac{W_{12}^2}{W_1 W_2} = \frac{g_{33}^2}{\beta^T_{33} s^D_{33}} . \tag{65}$$

---

[11] This can also be seen in Equation (9): For $k\ell = m(\pi/2)$ and m even, the voltage required to maintain vibration becomes infinite.

And for the dynamic case, of course,

$$\left.\begin{aligned}\frac{k_e^2}{1-k_e^2} &= \frac{[\int g_{33}\,DT\,dV]^2}{[\int \beta_{33}^T D^2\,dV][\int s_{33}^D T^2\,dV]} \\ &= \frac{k_{33}^2}{1-k_{33}^2}\;\frac{[\int DT\,dV]^2}{[\int D^2\,dV][\int T^2\,dV]}\end{aligned}\right\} \qquad (66)$$

The computation to evaluate this expression for the end-electroded bar turns out to be exactly the same form as that preceding Eq. (62), and the result is

$$\frac{k_e^2}{1-k_e^2} = \frac{k_{33}^2}{1-k_{33}^2}\left\{\frac{2\sin^2\kappa\ell}{\kappa\ell\,(\kappa\ell+\sin\kappa\ell\,\cos\kappa\ell)}\right\} . \qquad (67)$$

The results appear graphically as the dashed curve in Fig. 6 for $k_{33} = 0.64$. Note that as $\omega \to 0$ and the stress distribution in the bar flattens out, the expression in brackets has a limit of unity and again k_e (static) = k_{33}. Since the resonant frequency of the $\partial D/\partial x = 0$ bar is coupling-dependent (see Eq. (31)), it is difficult to evaluate Eq. (67) at resonance. The anti-resonant frequencies, though, are coupling-invariant and thus

$$\frac{k_e^2}{1-k_e^2} = \frac{8}{\pi^2}\;\frac{k_{33}^2}{1-k_{33}^2} \quad \text{at} \quad \kappa\ell = \frac{\pi}{2} .$$

Unlike the previous case there is no constant relationship for k_e/k_{33}.

For a specific k_{33}, however, one can evaluate k_e versus r by applying the above equation to Curve B in Fig. 4. The result is again graphically indistinguishable from Curve C. One may conclude, therefore, that Eq. (63) is valid for the experimental determination of the effective coupling of the unloaded end-electroded bar at anti-resonance.

This close approximation to the actual effective coupling by a simple formula is fortuitous. The reason for the agreement lies simply in the

fact that the effective stiffness of the transducer, though frequency-dependent, changes only slightly in the interval from resonance to anti-resonance. The variable r in Eq. (63) is obtained by measurements at two frequencies, while the value of coupling which results is associated with just one frequency. In lumped-constant circuits no difficulty is encountered by this since one constant value of coupling coefficient applies to all frequencies for which the circuit is valid — the distribution of state variables throughout the transducer is constant with frequency. When such constancy is not true, the measurement of the ratio of two separate frequencies may not be an adequate means of determining the coupling. The derivation of Eq. (63) rests on the assumption that the mechanical reactance of the transducer varies in a specific manner (i.e., that of a series L-C circuit), and the inclusion of reactances which vary according to some other scheme (e.g., a transcendental equation such as that in Fig. 2) destroys the validity of the derivation.

Although this discussion shows that the use of Eq. (63) will not produce exactly the correct value of effective coupling for some composite transducers, the equation still has great utility for comparative studies of a specific transducer. That is, although the numerical value of k_e obtained may be incorrect, one may quickly check the relative effect of design modifications on the coupling coefficient by using Eq. (63).

One further point of interest is that the effective coupling of the constant and variable field longitudinal vibrators diminishes at each successively higher overtone resonance. This is seen clearly in Eq. (62). for increasing $(k\ell)$ the numerator maintains the periodicity while the denominator causes the maxima of k_e to approach zero asymptotically. This phenomenon is due to the numerous nodes in the stress pattern at higher modes. It is evident from the definition given as Eq. (54) that the stress-field product should not vary greatly throughout the body in order to maintain high coupling.

This effect can sometimes be used to increase the effective coupling. Regions with full electrical excitation but low stress levels may be removed from the transducer. For instance, in flexural bars and plates, the low stresses near the neutral plane deteriorate the coupling.[12] If

[12] R. S. Woollett, "Theory of the Piezoelectric Flexural Disk Transducer with Applications to Underwater Sound," USL Research Report no. 490, S-F001 03 04-1, pp. 71-74, 1960.

these layers of ceramic are replaced by low-modulus inert material, the coupling may increase.

DYNAMIC COUPLING OF THE PARTIALLY EXCITED BAR

According to the definition of coupling used in this report, vibrations which do not directly participate in the electromechanical conversion process (i.e., are not electrically active) and static electrical elements which store electrical energy without being coupled to the vibrations through the piezoelectric effect (i.e., external capacitances) both tend to decrease the effective coupling coefficient of a transducer.

One example of this effect is the composite transducer in which an electromechanical driver excites other electrically inert, resonant, or non-resonant structures. A transducer coupled to a fluid-filled cavity is such a device; the effective coupling is lowered even if the cavity is tuned to have zero reactance at the natural resonance of the driver.

An experiment to test this principle has been performed by Toulis.[13] It consists of measuring the resonant and anti-resonant frequencies of a segmented multi-electroded stack of ceramic for varying degrees of electrical excitation. This experiment was described previously, and the frequency data appears in Fig. 5.

What is the theoretical dynamic coupling of such a partially excited structure from the energy-balance viewpoint? One finds immediately the electrical and mutual energies (in half the bar) to be

$$W_1(y) = \frac{1}{2}\epsilon_{33}^T A \int_0^{y\ell} \mathcal{E}_0^2 \, dx \tag{68}$$

and

$$W_{12}(y) = \frac{1}{2} d_{33} A \int_0^{y\ell} T_d \mathcal{E}_0 \, dx \ , \tag{69}$$

[13] Toulis, op. cit.

since $\mathcal{E}_f = 0$. The elastic energy, though, has two distinct parts: a contribution from the "d" section and one from the "f" section:

$$\left.\begin{aligned} W_2(y) &= \frac{1}{2} s^E_{33} A \int_0^{y\ell} T_d^2 \, dx + \frac{1}{2} s^D_{33} A \int_{y\ell}^{\ell} T_f^2 \, dx \\ &= U_d + U_f . \end{aligned}\right\} \tag{70}$$

By Eq. (54) the dynamic coupling of the composite bar is

$$k_e^2(y) = \frac{W_{12}^2}{W_1 (U_d + U_f)} = \frac{W_{12}^2}{W_1 U_d (1 + U_f/U_d)} . \tag{71}$$

Comparing Eq. (71) with the work on pages 19 and 20 reveals that $(W_{12}^2/W_1 U_d)^{1/2}$ is the effective coupling of a fully excited constant field bar of half length $y\ell$, while $(1 + U_f/U_d)$ is a correction term to account for the electrically inactive end sections of the partially excited bar.

Computation of the ratio U_f/U_d at system resonance as a function of y is tedious. The general form (that is, at all frequencies) is

$$\frac{U_f}{U_d} \quad \Xi(y) = \frac{\sin^2 y\Lambda_d \left[(1-y)\Lambda_f (1+\cot^2\Lambda_f) + (\sin\Lambda_f \cos\Lambda_f - \sin y\Lambda_f \cos y\Lambda_f)(1-\cot^2\Lambda_f) - 2\cot\Lambda_f (\sin^2\Lambda_f - \sin^2 y\Lambda_f)\right]}{\sqrt{1-k_{33}^2}\,(\sin y\Lambda_f + \cot\Lambda_f \cos y\Lambda_f)^2 (y\Lambda_d + \sin y\Lambda_d \cos y\Lambda_d)} . \tag{72}$$

To find the effective coupling at the fundamental resonance as a function of y, one solves Eq. (43) for the resonance parameters $\Lambda_d^E(y)$, forms the functions

$$\Lambda_f^E = \sqrt{1-k_{33}^2}\ \Lambda_d^E , \tag{73}$$

and evaluates $\Xi(y)$ from Eq. (72).

The coupling is

$$k_e(\gamma) = \left\{ \frac{2k_{33}^2}{\gamma \Lambda_d (\gamma \Lambda_d \cos^2 \gamma \Lambda_d + \cot \gamma \Lambda_d)(1 + \Xi)} \right\}^{1/2} . \qquad (74)$$

These computations were performed on a digital computer; the results appear in Fig. 7 for various values of k_{33}.

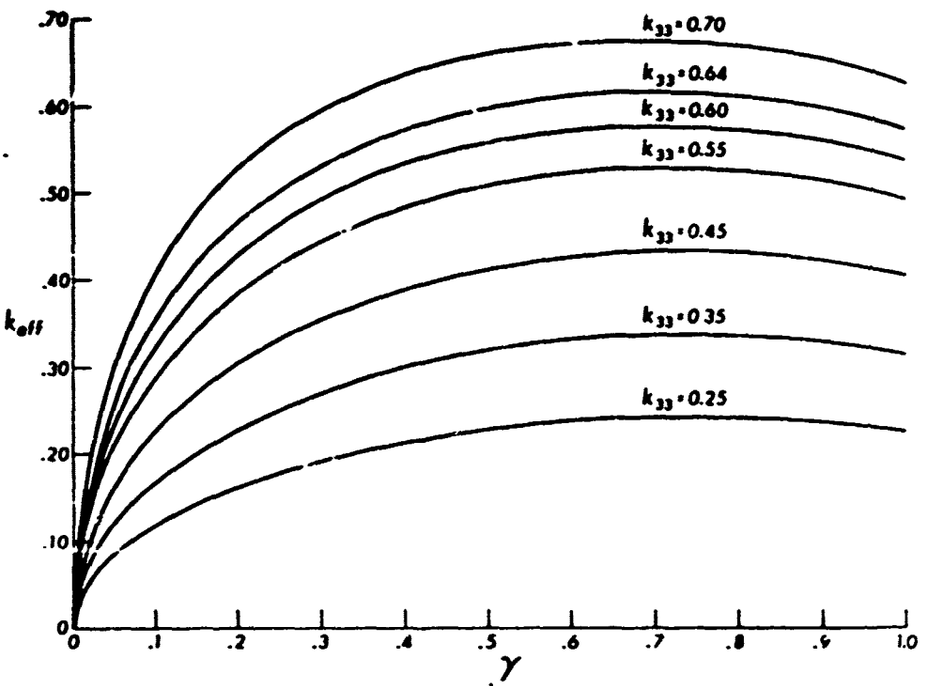

Fig. 7 - Effective Coupling of a Partially Excited Stack as a Function of Degree of Excitation for Various Values of k_{33}

The relative maximum of $k_e(\gamma)$ near $\gamma = 0.7$ results because the mass loading of the electrically active central part by the unexcited end sections causes the stress distribution to become less severe and raises the coupling. For small γ, however, the large amounts of strain energy in the end sections lowers the system coupling again.

The simple formula Eq. (63) becomes, in the notation of this problem,

$$k^2 = 1 - (\delta^E / \epsilon \delta^S)^2 . \qquad (75)$$

Once again this approximate expression is sufficiently accurate for good engineering over all of the range of k_{33} presently availabie (less than 1 percent error for all γ and all $k_{33} \leq 0.65$).

Applying Eq. (75) to Toulis' data (Fig. 5) produces the experimental coupling versus γ points plotted in Fig. 8. The theoretical curve for $k_{33} = 0.64$ is also drawn for comparison (solid curve). An earlier study of a partially excited, side-electroded bar was made by Beckmann and Parsons.[14] Although their treatment was simplified by neglecting the change of elastic properties of the material between the active and inactive regions, the general shape is similar (Fig. 8, dashed line).

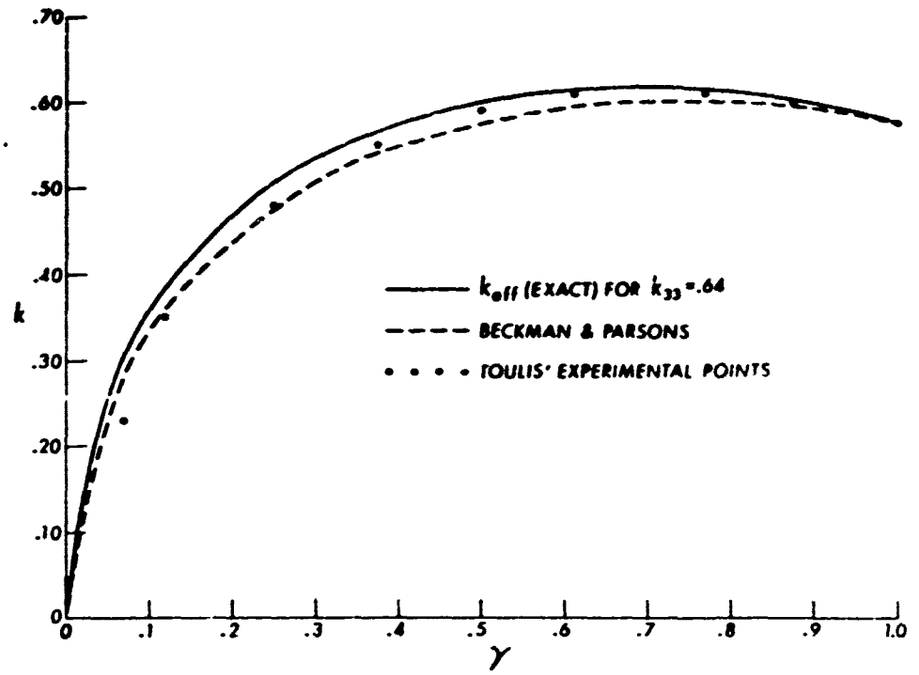

Fig. 8 - Dynamic Coupling Coefficient of the Partially Excited Bar versus γ

[14] R. Beckmann and P. L. Parson, Piezoelectricity, H. M. Stationery Office, London, p. 296, 1957.

Navy Underwater Sound Laboratory
Report No. 622
DYNAMIC COUPLING COEFFICIENTS FOR DISTRIBUTED PARAMETER PIEZOELECTRIC TRANSDUCERS, by William J. Marshall 16 October 1964
i-ii + 28 p., figs. UNCLASSIFIED

This report discusses a definition of the effective coupling coefficient for the body-force class of electromechanical transducers. This definition is based on the distribution of energy in the transducer and is therefore particularly applicable to the "distributed parameter" type of transducer. Furthermore, the definition results in a frequency dependent coupling coefficient which is valid for all modes of vibration.

The definition is applied to some common types of longitudinal vibrator and the results are compared with experiments for one particular device (a partially excited stack of ceramic disks). The influence of parasitic elements on the system coupling is also examined.

1. Piezoelectric transducers
2. Magnetostrictive transducers
3. Vibrators (electrical)
4. Coupling coefficient
I. Marshall, William J.
II. Title
III. S-F001 03 18-8044

Navy Underwater Sound Laboratory
Report No. 622
DYNAMIC COUPLING COEFFICIENTS FOR DISTRIBUTED PARAMETER PIEZOELECTRIC TRANSDUCERS, by William J. Marshall 16 October 1964
i-ii + 28 p., figs. UNCLASSIFIED

This report discusses a definition of the effective coupling coefficient for the body-force class of electromechanical transducers. This definition is based on the distribution of energy in the transducer and is therefore particularly applicable to the "distributed parameter" type of transducer. Furthermore, the definition results in a frequency dependent coupling coefficient which is valid for all modes of vibration.

The definition is applied to some common types of longitudinal vibrator and the results are compared with experiments for one particular device (a partially excited stack of ceramic disks). The influence of parasitic elements on the system coupling is also examined.

1. Piezoelectric transducers
2. Magnetostrictive transducers
3. Vibrators (electrical)
4. Coupling coefficient
I. Marshall, William J.
II. Title
III. S-F001 03 18-8044

DISTRIBUTION LIST

Chief of Naval Operations, Op-07T (2)
Bureau of Ships, Code 210L (3)
Code 320
Code 333
Code 1622
Bureau of Naval Weapons, Library
Office of Naval Research, Code 411
Code 466
Commander, Operational Test and Evaluation Force
Commander, Operational Test and Evaluation Force, Undersea Warfare Division
U. S. Naval Air Development Center
U. S. Naval Ordnance Laboratory
U. S. Naval Research Laboratory
U. S. Navy Electronics Laboratory
U. S. Navy Mine Defense Laboratory
Applied Physics Laboratory, University of Washington
David Taylor Model Basin
Hudson Laboratories, Columbia University
Marine Physical Laboratory, Scripps Institution of Oceanography
Ordnance Research Laboratory, Pennsylvania State University
Systems Analysis Group, Research and Development Planning Council,
U. S. Naval Ordnance Laboratory
Woods Hole Oceanographic Institution
U. S. Naval Avionics Facility
U. S. Navy Marine Engineering Laboratory
U. S. Navy Underwater Sound Reference Laboratory
U. S. Naval Applied Science Laboratory
U. S. Naval Postgraduate School
Committee on Undersea Warfare, National Research Council
Defense Documentation Center (DDC) (20)